การจำลองพลวัตเชิงโมเลกุลและการคำนวณทางเคมีควอนตัมของยาเกมซาร์ในท่อนาโนคาร์บอน
ผนังเดี่ยวที่มีการดัดแปรผิว

นางสาวอุทุมพร อาสว่าง

Molecular Dynamics Simulations and Quantum Chemical Calculations of GEMZAR
in Surface-Modified Carbon Nanotube

Miss Uthumporn Arsawang

ศูนย์วิทยทรัพยากร
จุฬาลงกรณ์มหาวิทยาลัย

A Thesis Submitted in Partial Fulfillment of the Requirements
for the Degree of Master of Science Program in Computational Science
Department of Mathematics
Faculty of Science
Chulalongkorn University
Academic Year 2009

Thesis Title      MOLECULAR DYNAMICS SIMULATIONS AND
QUANTUM CHEMICAL CALCULATIONS OF GEMZAR
IN SURFACE-MODIFIED CARBON NANOTUBE

By      Miss Uthumporn Arsawang

Field of Study      Computational Science

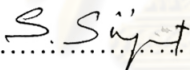Thesis Advisor      Professor Supot Hannongbua, Dr.rer.nat.

Thesis Co-Advisor      Assistant Professor Tawun Remsungnen, Dr.rer.nat.

---

Accepted by the Faculty of Science, Chulalongkorn University in Partial Fulfillment of the Requirements for the Master's Degree

.....................................Dean of the Faculty of Science

(Professor Supot Hannongbua, Dr.rer.nat.)

THESIS COMMITTEE
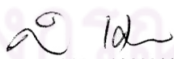
............................................. Chairman

(Associate Professor Suchada Siripant)
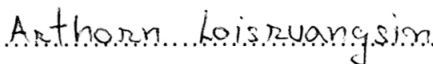
............................................. Thesis Advisor

(Professor Supot Hannongbua, Dr.rer.nat.)

............................................. Thesis Co-Advisor

(Assistant Professor Tawun Remsungnen, Dr.rer.nat.)

............................................. Examiner

(Khamron Mekchay, Ph.D.)

............................................. External Examiner

(Arthorn Loisruangsin, Ph.D.)

อุทุมพร อาสว่าง: การจำลองพลวัตเชิงโมเลกุลและการคำนวณเคมีควอนตัมของ ยาเกมซาร์ในท่อนาโนคาร์บอนผนังเดี่ยวที่มีการดัดแปรผิว. (MOLECULAR DYNAMICS SIMULATIONS AND QUANTUM CHEMICAL CALCULATIONS OF GEMZAR IN SURFACE-MODIFIED CARBON NANOTUBE) อ.ที่ปรึกษา วิทยานิพนธ์หลัก: ศ.ดร. สุพจน์ หารหนองบัว, อ.ที่ปรึกษาวิทยานิพนธ์ร่วม: ผศ.ดร. เทวัญ เริ่มสูงเนิน 53 หน้า.


จุดมุ่งหมายหลักของงานวิจัยนี้คือการทำความเข้าใจในระดับโมเลกุลของการนำส่งยา ต้านมะเร็งด้วยท่อนาโนคาร์บอนผนังเดี่ยวและท่อนาโนคาร์บอนผนังเดี่ยวที่มีการดัดแปรผิว ด้วยหมู่ฟังก์ชันกรดคาร์บอกซิลลิกและเบสไฮดรอกซิล ในขั้นแรกได้คำนวณโครงสร้างของท่อ นาโนคาร์บอนโดยใช้ระเบียบวิธีการคำนวณเคมีควอนตัม ซึ่งศึกษาในระบบของท่อนาโน คาร์บอนและท่อนาโนคาร์บอนที่มีการดัดแปรผิว ผลการทดลองระบุว่าการเติมหมู่ฟังก์ชันที่ ผนังท่อมีผลทำให้ความแบนราบของผิวท่อลดลง จากนั้นทำการทดลองโดยวิธีจำลองพลวัตเชิง โมเลกุล โดยระบบที่ศึกษาประกอบด้วยยาเกมซิตาบีนในน้ำและในท่อนาโนคาร์บอนผนังเดี่ยว ผลการศึกษาพบว่า ยาสามารถเคลื่อนที่ได้อย่างอิสระจากปลายด้านหนึ่งไปยังปลายอีกด้านหนึ่ง ของท่อขนานไปกับแนวผนังท่อโดยที่วงไซโตซีนทำมุม 19 องศากับผนังท่อซึ่งถือว่าเป็นการ วางตัวแบบอะโรมาติกแสต็กกิง และเมื่อพิจารณาในแนวตั้งฉากกับผนังท่อพบว่า ยาวางตัวห่าง จากผนังท่อเป็นระยะประมาณ 4.7 อังสตรอม นอกจากนี้สมบัติทางโครงสร้างของตัวยาซึ่ง พิจารณาการวางตัวของวงไซโตซีนและวงไรโบสพบว่ายาเกมซาร์เมื่ออยู่ในน้ำและในท่อนาโน คาร์บอน ทั้งที่ระบบที่ยาอยู่ในท่อจะถูกกล้อมรอบด้วยน้ำได้อ่อนแรงกว่าและมีจำนวนโมเลกุล น้ำอยู่โดยรอบน้อยกว่าระบบที่ยาอยู่เดี่ยวๆ นอกจากนี้ยังมีการศึกษาระบบของยาเกมซิตาบีนใน ท่อนาโนคาร์บอนผนังเดี่ยวที่มีการดัดแปรผิวด้วยหมู่ฟังก์ชันกรดคาร์บอกซิลลิกและกรดคาร์ บอกซิลลิก จากผลการทดลองพบว่าไม่มีความแตกต่างสำหรับระบบของท่อที่ไม่มีการดัดแปร ผิวและที่มีการดัดแปรผิว

| ภาควิชา | คณิตศาสตร์ | ลายมือชื่อนิสิต | อุทุมพร อาสว่าง |
| --- | --- | --- | --- |
| สาขาวิชา | วิทยาการคณนา | ลายมือชื่อ อ.ที่ปรึกษาวิทยานิพนธ์หลัก | |
| ปีการศึกษา | 2552 | ลายมือชื่อ อ.ที่ปรึกษาวิทยานิพนธ์ร่วม | |

# # 4972583323 : MAJOR COMPUTATIONAL SCIENCE

KEYWORDS : CARBON NANOTUBE / GEMZAR / DRUG DELIVERY / QUANTUM CHEMICAL CALCULATIONS / MOLECULAR DYNAMICS SIMULATIONS

> UTHUMPORN ARSAWANG: MOLECULAR DYNAMICS SIMULATIONS AND QUANTUM CHEMICAL CALCULATIONS OF GEMZAR IN SURFACE-MODIFIED CARBON NANOTUBE. THESIS ADVISOR: PROF. SUPOT HANNONGBUA, Dr.rer.nat., THESIS CO-ADVISOR: ASSIST.PROF. TAWUN REMSUNGNEN, Dr.rer.nat., 53 pp.

Understanding of molecular properties of the encapsulation of the GEMZAR anticancer drug in the single-walled carbon nanotube (SWCNT) is the main goal of this study. The molecular geometries of the pristine and functionalized SWCNTs were studied by the simiempirical PM3 method. It was found that modification on the outer surface of the tube by the –COOH and –OH functional groups leads to the lowered planarity of the tube surface. Then, MD simulations were applied to investigate structural and dynamical properties of the GEMZAR in free and the pristine SWCNT bound states. As a result, the drug was found to move freely from one end to the other of the SWCNT, not along the tube axis at the center of the tube but parallel at the distance of 4.7 Å from the inner surface. Using the structural data, the angle between the cytosine-based and the inner surface of $19^{\circ}$ was yielded, indicating that the drug always positioned inside the tube and partially interacted with the surface through the aromatic stacking interaction. The most probable conformation of the cytosine-based and ribose rings in both states was relatively similar. In addition, drug molecule was weaker and less solvated in which the SWCNT than that of the free state because of the collaborative interaction with the inner surface of the tube. Furthermore, overall drug properties inside the functionalized SWCNTs modified by the –COOH and –OH groups were considerably similar to what observed for the pristine SWCNT.

Department : Mathematics          Student's Signature Uthumporn Arsawang

Field of Study : Computational Science     Advisor's Signature S. Hannongbua

Academic Year : 2009          Co-Advisor's Signature Tawun Rem

# ACKNOWLEDGEMENTS

Firstly, I would like to thank my family for all their love, encouragement and support. I owe my deepest gratitude to my benevolence advisor, Prof. Dr.rer.nat. Supot Hannongbua, who always gives me a new idea and never complain me in my mistakes. Besides, he spent his time to take care my thesis despite he has a lot of works in his position. Moreover, I am grateful thank to Assist. Prof. Dr.rer.nat. Tawun Remsungnen, who had gave me help and suggestions while I stayed in Khon Kaen University. Moreover, this thesis would not have been possible unless I obtain kindheartedness help and suggest from Dr. Thanyada Rungrotmongkol and Dr. Oraphan Saengsawang.

I would like to special thanks to Assoc. Prof. Dr. Suchada Siripant, Dr. Khamron Mekchay and Dr. Arthorn Loisruangsin who act as the thesis committee.

I thank all of my friends especially, Miss Chalalai Poree who always cheers me up. It is an honor for me to accompany with Miss Purinchaya Sornmee. I am heartily thankful to Mr. Naphattharaphong Prasertsri who helps me in computer graphic programming. For CCUC members, I appreciate for many help in works and for happiness lifestyles.

Finally, I am grateful to the Computational Chemistry Unit Cell (CCUC) at Chulalongkorn University and the HPC service at National Electronics and Computer Technology Center (NECTEC) for computer resources and other facilities. I am also grateful to the Development and Promotion of Science and technology Talents project (DPST) and the graduate school Chulalongkorn University for financial support during the study.

It is a pleasure to thank those who made this thesis possible.

# CONTENTS

# LIST OF TABLES

# LIST OF FIGURES

# LIST OF ABBREVIATIONS

| | | |
|---|---|---|
| CNTs | = | Carbon nanotubes |
| SWCNTs | = | Single-walled carbon nanotubes |
| MWCNTs | = | Multi-walled carbon nanotubes |
| CDC | = | The Centers for Disease Control and Prevention |
| QM | = | Quantum Chemical Culations |
| MD | = | Molecular Dynamics Simulations |
| PDB | = | Protein Data Bank |
| HF | = | Hartree-Fock |
| ESP | = | Electrostatic potentials |
| RESP | = | Restricted Electrostatic potentials |
| GAFF | = | The Generalized AMBER Force Field |
| $Cg$ | = | The center of gravity |
| $d(Cg)$ | = | displacement $Cg$ of drug |
| $P(Cg)$ | = | The probability of finding the $Cg$ of drug molecule |
| RDFs | = | The atom-atom radial distribution functions |
| $CN$ | = | Coordination number |

# CHAPTER I

# INTRODUCTION

## 1.1.    Research Rationale

Since the breakthrough in discovery of the carbon nanotubes (CNTs) in 1991 [1], they have been considered as the ideal materials for a variety of applications. One of those is to be used in the nanomedicine research for the reason that they are biocompatible in pharmaceutical drug delivery systems [2-4]. Nowadays, experimental and theoretical researches usually target to improve CNT to be an excellent drug carrier with highly site-selective delivery and sensitivity [5-10]. Understanding at the molecular level of how the single-walled carbon nanotube (SWCNT) carries out a drug as well as the structural and dynamics properties of the drug-SWCNT complex is a key of success in designing and developing the newly effective drug transporter for the drug delivery system. This becomes the rationale goal of this study.

## 1.2.    Carbon Nanotubes

Carbon nanotubes are the nanoscale materials which its structures were extended in length of the fullerene (Fig. 1.1). It is often stated that the structure of the CNT is the graphene sheet which rolled up into the cylinder as in Fig. 1.2
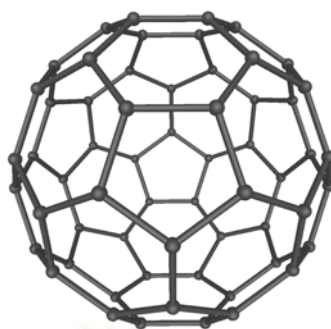
**Figure 1.1** The structure of the buckyball C60 or the fullerene.
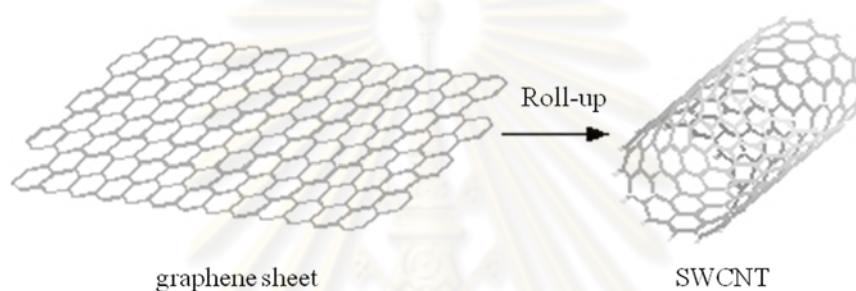


**Figure 1.2** The rolled up process of graphene sheet to the single-walled carbon nanotube.

The CNTs are categorized as single-walled carbon nanotubes (SWCNTs) and multi-walled carbon nanotubes (MWCNTs). They can be classified into three types by two wrapping directions, $\vec{a}_1$ and $\vec{a}_2$, which are called the 'chiral vector'.
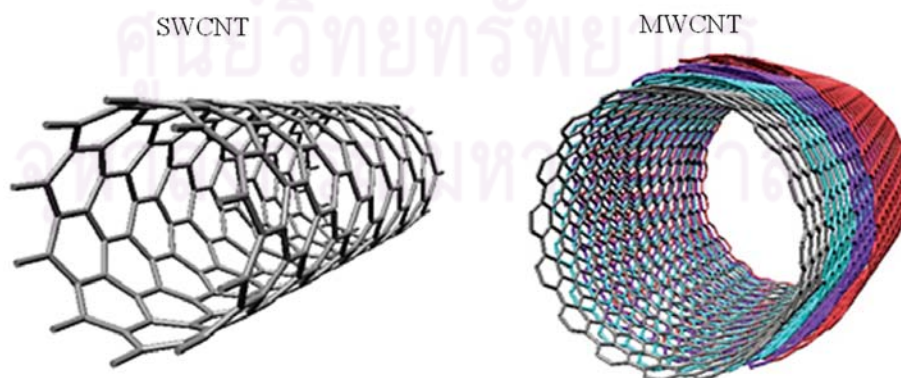


**Figure 1.3** The single-walled and multi-walled carbon nanotubes, SWCNT and MWCNT.
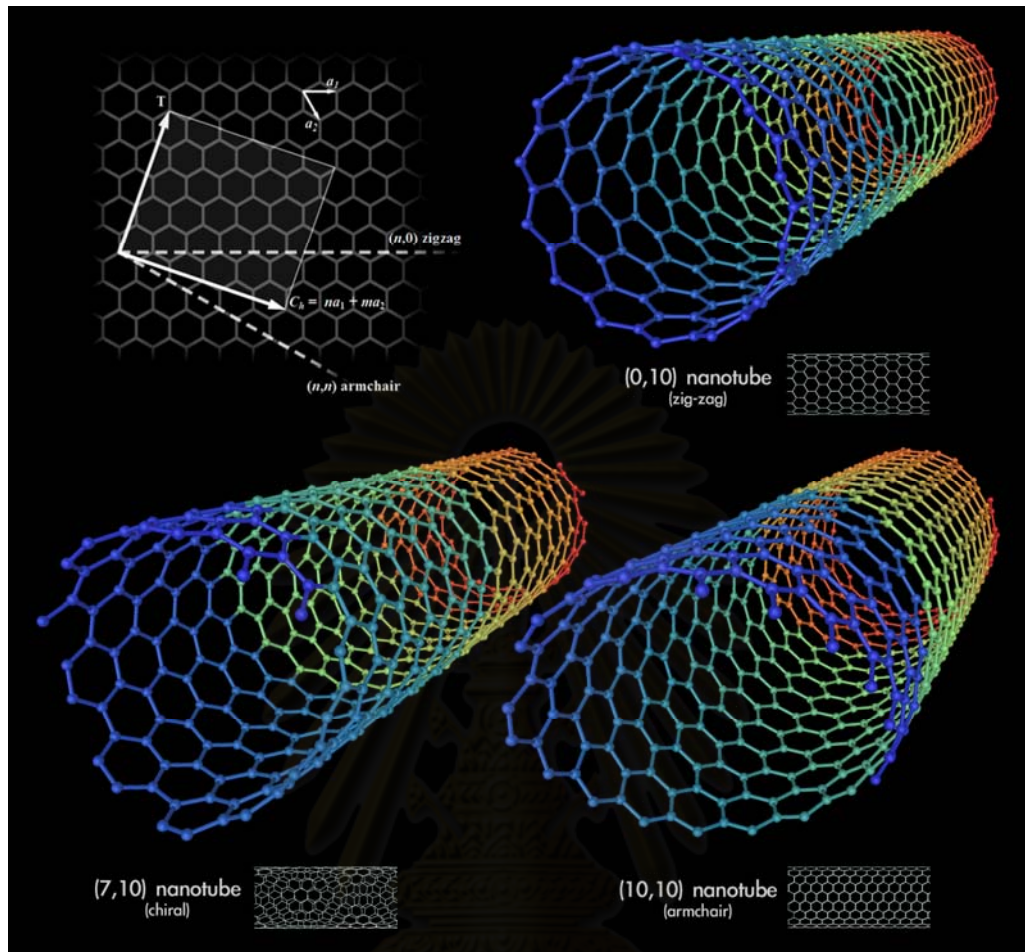
**Figure 1.4** Three types of SWCNTs classified by the 'chiral vector'.

According to the chiral equation of CNTs, $\vec{C}_h = n\vec{a}_1 + m\vec{a}_2$, three types of CNTs namely zigzag, armchair and chiral CNTs can be formed. The one-direction-rolled graphene sheet is called 'zigzag' CNTs. The armchair-liked cross section CNTs is named 'armchair' CNTs which the direction of rolling is $\vec{a}_1 = \vec{a}_2$. The other type of rolling up leads to the 'chiral' CNTs.

## 1.3. Functionalized Carbon Nanotubes

With the hydrophobic surface, the non-functionalized CNTs (or pristine CNTs) are difficult to be solvated by the hydrophilic solvents, causing the toxicity of the CNTs.

Many researchers have been focused on trying to modify their surface to reduce these disadvantage properties. The CNTs that are attached the molecules or the functional groups at their surface or even at both ends, are called functionalized CNTs. This modification causes reduce the toxicity of CNTs.

## 1.4.    Applications of Carbon Nanotubes

Since CNTs are unique materials, not only small size but also the incredibly physical properties, the CNTs have attracted many scientists worldwide. They are applied as the nano-electronic, nano-gear, nano-composite, nano-sensor devices etc. and the pharmaceutical drug delivery systems as mentioned above. The latter is the most useful application of CNTs.

## 1.5.    Carbon Nanotubes as Drug delivery

The Centers for Disease Control and Prevention (CDC) reported cancer as the second leading cause in the number of deaths worldwide. Among the various types of cancer, the ovarian cancer is the fifth most common cancer in people and extremely causes of deaths in women more than other types of cancer found in the female reproductive malignant cells. Gemcitabine is an anti-cancer drug used in combination with carboplatin to treat the ovarian cancer. It could prevent the further growth of cancer cells and cause of the cell death by interrupting the production of the genetic materials including DNA and RNA. The main problem from any cancer treatment and therapy is the serious side effects to the normal cells. The bone marrow toxicity can be affected in the patients who are allergic to gemcitabine. To avoid such effects, the development of

drug delivery system is required to transport the drug molecules efficiently and specifically to the targeted tumor cells, without harming the surrounding tissue.

### 1.5.1. Ovarian Cancer

Ovarian cancer is a type of cancers, growing from different parts of the ovary in which more than 90 % is the epithelial type. The ovaries breed eggs for reproduction and female hormones causing the uncontrollably dividing cells in women. The exact origin of this cancer is unknown and the symptoms often only appear in the later stages. These tumors are hardly detected during a physical exam, as a result, about 70 % of patients are found with advanced disease. Since it is the non-specific symptoms cancer, the diagnosis of ovarian cancer often start with physical examinations and must be confirmed with surgery. The treatment generally involves surgery and chemotherapy. In addition, some patients may need the radiotherapy with participation. The gemcitabine (or trade name as GEMZAR®) and the carboplatin drugs are used to cure this cancer.
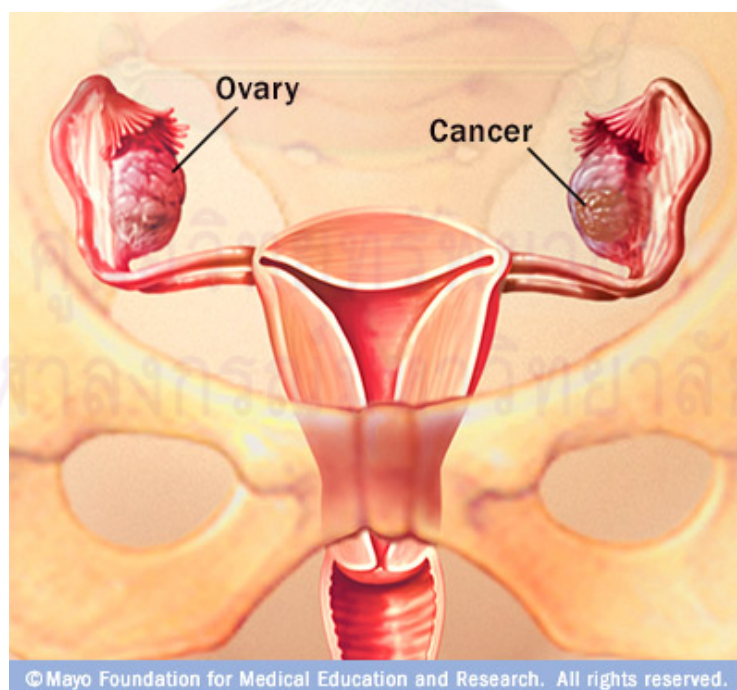
**Figure 1.5** The typical ovary and the cancer ovary.

### 1.5.2. GEMZAR® (gemcitabine HCl)

GEMZAR® (gemcitabine HCl for injection) is the one of the anti-cancer drugs used to help the ovarian cancer patients. It is cytidine-like drug in which the hydrogen atoms on the 2' carbon of deoxycytidine are replaced by fluorine atoms. The drug function is building block of cytidine, a nucleic acid, during DNA replication. As a result, the faulty nucleosides are found, resulting the apoptosis. In addition, the enzyme namely ribonucleotide reductase (RNR) is also the target of gemcitabine. The diphosphate analogue inhibits the RNR by binding at the active site and inactivating the enzyme irreversibly. Resultingly, the cell apoptosis is induced, because the deoxyribonucleotide required for DNA replication and repair cannot be produced.
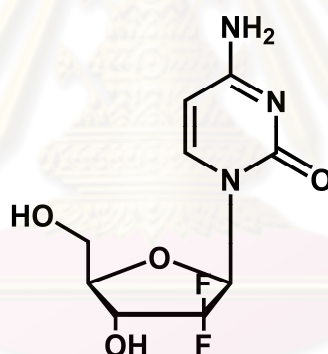


**Figure 1.6** The 2D structure of GEMZAR® drug.

The drug can be used as a single agent (given alone) with the first-line treatment for the pancreatic cancer patients, or in combination with other therapies. The combination with cisplatin is used for first-line treatment of patients with locally advanced or metastatic non-small cell lung cancer for whom surgery is not possible, or with paclitaxel for the first-line treatment of patients with metastatic breast cancer after they have received another type of chemotherapy. After the patients had finished the platinum-based therapy (gemcitabine and carboplatin), they recovered at least 6 months.

By cancer treatments and therapies, there may cause many side effect of the drug. The common side effects are low blood cell counts, hair loss, tiredness, nausea, vomiting, and constipation. The GEMZAR[®] may suppress bone marrow function for allergic patient or even the women who think or plan to become pregnant.

Gemcitabine is an anti-cancer drug used in combination with carboplatin to treat the ovarian cancer. It could prevent the further growth of cancer cells and cause of the cell death by interrupting the production of the genetic materials including DNA and RNA. The main problem from any cancer treatment and therapy is the serious side effects to the normal cells. The bone marrow toxicity can be affected in the patients who are allergic to gemcitabine. To avoid such effects, the development of drug delivery system is required to transport the drug molecules efficiently and specifically to the targeted tumor cells, without harming the surrounding tissue.

## 1.6. Literature Review on Drug Delivery System

Many experimental studies have demonstrated that CNTs show the carrier properties by serving as a transporter of bio-molecules to the target site including drugs [11-15], vaccines [16-17], small peptides [18-19], proteins [20-23] and nucleic acids [24-26]. Basically, these molecules attach on either inner or outer tube wall surfaces, so-called filling or wrapping modes of binding. The functionalization of SWCNTs was found to reduce the toxic nature of the non-functionalized pristine SWCNT *in vitro* and *in vivo* applications [27-29].

### 1.6.1. Quantum Chemical Calculation

The functionalized SWCNTs have been studied using the quantum chemical (QM) calculations to describe the properties. The diameter dependent possible positions

of functional groups on SWCNT have been reported by Kuzmany *et al.* [30] in 2004. In the same year, Zhao *et al.* [31] has published the electronic states near the Fermi level which told us that functional group can induces an impurity state. The functional groups are attached at the surface of the tube for improving the SWCNT more biocompatibility [32].

### 1.6.2. Molecular Dynamics Simulation

The molecular dynamics (MD) simulation has been used to study the structural and dynamics properties of SWCNTs. The series of water profile inside the SWCNTs were reported in many years ago [33-40]. Based on their studies, different force fields and water models bring different set of data.

The functionalized inside CNTs has been proposed by Zheng *et al.* [41], they found that the transport of liquid mixture through inner hydrophilic part is slower than the outside. The effect of functional groups on the structural water molecules had resulted to the cooperation effects of the CNTs' helicity and diameter and controlling the flow direction of water molecules in CNTs [42-43]. Recently, Zhu *et al.* [44] have found that the number of the functionalized –COOH groups on the inner surface of the CNT affected to the density distribution of water molecules.

From the MD simulation of DNA-CNT complex, the encapsulation was suggested for further applications [46]. The molecular dynamics (MD) simulation of Vitamin A and β-Carotene encapsulated in CNTs have been studied [47]. Under different conditions of nanotube wall number, chirality, radius and temperature both of them were found to be the promising biomaterials for decoration of CNTs which are in good agreement with the experiments data [23,46].

## 1.7. The Objective of Study

The present study has focused upon trying to reveal the drug binding inside the three different SWCNTs: a pristine and two functionalized tubes with the carboxylic acid and hydroxyl groups on the outer surface of the tube. Molecular geometries of the SWCNTs were optimized using quantum chemical calculations. The free and SWCNT bound states of gemcitabine were individually set up and performed by molecular dynamics simulations. The drug-CNT interactions and the ligand structural, dynamics and solvation properties were analyzed and extensively discussed. This technique has been successfully used to investigate the intermolecular interactions between CNTs and the other biological molecules such as DNA [46], Vitamin A and β-Carotene [47], and amylose [48].

# CHAPTER II

# THEORY BACKGROUND

In this chapter, the basic knowledge of calculation method used in this work is provided. The details of two main methods utilized based on mathematic description including quantum chemistry method and molecular dynamic simulations are briefly given.

## 2.1    Quantum Chemistry Calculations

### 2.1.1    Quantum mechanics

Quantum mechanics (QM) [49] is the correct mathematical description of the behavior of electrons and thus of chemistry. In theory, QM can predict any property of an individual atom or molecule exactly. In practice, the QM equations have only been solved exactly for one electron systems. A numerous collection of methods has been developed for approximating the solution for multiple electron systems. These approximations can be very useful, but this requires an amount of sophistication on the part of the researcher to know when each approximation is valid and how accurate the results are likely to be.

The basic equation that used in QM is the Schrödinger equation which shown in equation [2.1]

$$\hat{H}\Psi \;=\; E\Psi \qquad\qquad [2.1]$$

where $\hat{H}$ is the Hamiltonian operator, $\Psi$ the wave function, and $E$ the energy. In the language of mathematics, an equation of this form is called and eigen equation. $\Psi$ is then called the eigenfunction and $E$ is an eigenvalue. The operator and eigenfunction can be a matrix and vector, respectively, but this is not always the case.

The wave function $\Psi$ is a function of the electron and nuclear positions. As the name implies, this is the description of an electron as a wave. This is a probabilistic description of electron behavior. As such, it can describe the probability of electrons being in certain locations, but it cannot predict exactly where electrons are located. The wave function is also called probability amplitude because it is the square of the wave function that yields probabilities. This is the only carefully correct meaning of a wave function. In order to obtain a physically relevant solution of the Schrödinger equation, the wave function must be continuous, single-valued, normalized, and anti-symmetrical with respect to the interchange of electrons.

### 2.1.2 *Ab initio* methods

The term *ab initio* is Latin for "from the beginning". This name is given to computations that are derived directly from theoretical principles with no inclusion of experimental data. This is an approximate quantum mechanical calculation. The approximations made are usually mathematical approximations, such as using a simpler functional form for a function or finding an approximate solution to a differential equation.

All molecular wave functions are approximate; some are just more approximate than others. We can solve the Schrödinger equation exactly for the hydrogen atom.

### 2.1.3  Semi-empirical Calculation

Semi-empirical methods increase the speed of computation by using approximations of *ab initio* techniques (*e.g.,* by limiting choices of molecular orbital or considering only valence electrons) which have been fitted to experimental data (for instance, structures and formation energies of organic molecules). Until recently, the size of many energetic molecules placed them beyond the scope of *ab initio* calculations. However, semi-empirical methods have been calibrated to typical organic or biological systems and tend to be inaccurate for problems involving hydrogen-bonding, chemical transitions or nitrated compounds. Some of the more common semi-empirical methods can be grouped according to their treatment of electron-electron interactions, *such as*, AM1 and PM3 method.

The PM3 Hamiltonian contains essentially the same elements as that for AM1, but the parameters for the PM3 model were derived using an automated parameterization procedure. By contrast, many of the parameters in AM1 were obtained by applying chemical knowledge and 'instinct'. As a consequence, some of the parameters have significantly different values in AM1 and PM3, even though both methods use the same functional form and they both predict various thermodynamic and structural properties to approximately the same level of accuracy.  Some problems do remain with PM3.  One of the most important of these is the rotational barrier of the amide bond, which is much too low and in some cases almost non-existent.  This problem can be corrected through the use of an empirical torsional potential.  There has been considerable debate over the relative merits of the AM1 and PM3 approaches to parameterization.

## 2.2 Intramolecular and Intermolecular potential functions

The investigation of the relationships between structures, function and dynamics at the atomic level can be expressed by giving the potential energy function, which can provide from the summation of the intramolecular and the intermolecular potential functions. In generally, the potential energy function is

$$V(R) = V_{bonded}(R) + V_{non-bonded}(R) \qquad [2.2]$$

### 2.2.1 Intramolecular potential functions

The intramolecular potential functions are the potential energy functions that used to describe the bonded behavior of atoms in the molecules by looking at the bonds as springs, expressed as the bonds stretching, the bond angles, and the dihedral (torsion) angles (Fig. 2.1). The equation of intramolecular is shown in equation [2.3]

$$V_{bonded}(R) = E_{bond-stretch} + E_{angle-bend} + E_{torsion-angle} \qquad [2.3]$$

#### 2.2.1.1 Bonds stretching ($E_{bond-stretch}$)
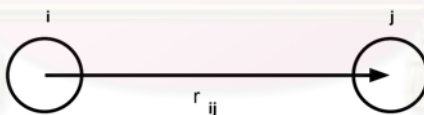


**Figure 2.1** The bond interaction between two atoms.

The harmonic interaction between two atoms which bonded directly (Fig. 2.1) to each other is used to describe the stretching of bond as in the equations [2.4]

$$E_{bond-stretch} = \sum_{i=1}^{n} k_b (r_{ij} - r_0)^2 \qquad [2.4]$$

where $r_{ij}$ is the length of bond between atoms $i$ and $j$ (Å),

$r_0$ is the equilibrium length of bond (Å),

$k_b$ is the constant of bond stretching (kcal·mol$^{-1}$(Å)$^2$).

### 2.2.1.2 Bond angles ( $E_{angle-bend}$ )
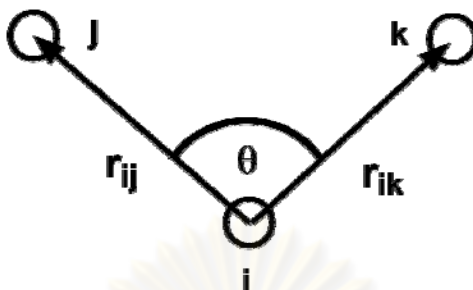


**Figure 2.2** The angle between two connected bonds.

      The harmonic interaction of two connected bonds can be described as the function of angular displacement. The equation of this interaction is

$$E_{angle-bend} = \sum_{i=1}^{n} k_\theta (\theta_{ijk} - \theta_0)^2 \qquad [2.5]$$

where   $\theta_{ijk}$     is the angle between two connected bonds (degree),

        $\theta_0$     is the equilibrium angle (degree),

        $k_\theta$     is the constant of angle bending (kcal·mol$^{-1}$(degree)$^2$).

### 2.2.1.3 Dihedral (Torsion) angles ( $E_{torsion-angle}$ )
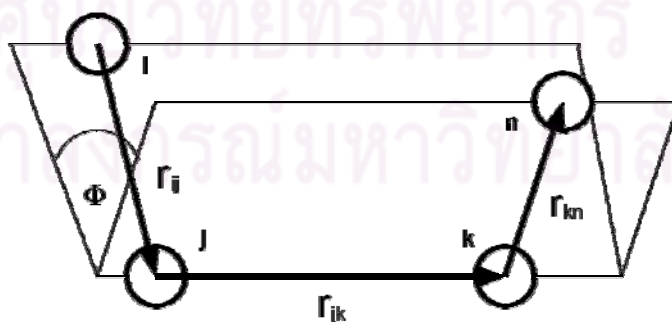


**Figure 2.3** The torsion angle represented as $\phi$ .

The dihedral angles or torsion angles are the twisted angle between two planes of three connected atom which has two atoms that same to the other. The interaction of the dihedral angles is treated as a cosine series and modeled by a simply periodic function as

$$E_{torsion-angle} = \sum_{1,4\,pair} k_\phi [1 - \cos(n\phi_{ijkn})]$$ [2.6]

where $\phi_{ijkn}$     is the torsional angle (degree),

      $n$       is the periodicity,

      $k_\phi$       is the constant of torsional barrier (kcal·mol$^{-1}$).

### 2.2.2 Intermolecular potential functions

The non-bonded potential functions were explained in term of intermolecular potential functions. In generally, in can be contributed by two functions which are van der Waals interaction energy and electrostatic interaction energy. The equation that used to describe this potential functions is

$$V_{non-bonded}(R) = E_{vdw} + E_{electrostatic}$$ [2.7]

where $E_{vdw}$ is the van der Waals interaction energy, and $E_{electrostatic}$ is the interaction distribution of the electron.

The van der Waals interaction between two atoms arises from a balance between repulsive and attractive forces. The equation of this interaction is written as the Lennard-Jones potential [78]

$$E_{LJ} = \varepsilon_{ij} \left[ \left( \frac{\sigma_{ij}}{r_{ij}} \right)^{12} - \left( \frac{\sigma_{ij}}{r_{ij}} \right)^{6} \right]$$ [2.8]

where $\varepsilon_{ij}$     is the well depth of energy (kcal),

      $\sigma_{ij}$       is the diameter (Å),

$r_{ij}$    is the distance between two atoms (Å).

The term of $r^{12}$ is represented as the repulsive part while the attractive part is given by the term of $r^6$. The $\varepsilon_{ij}$ and $\sigma_{ij}$ can be calculated from the combinatorial equation [79]

$$\varepsilon_{ij} = \sqrt{\varepsilon_i \varepsilon_j} \qquad\qquad [2.9]$$

$$\sigma_{ij} = \frac{\sigma_i + \sigma_j}{2} \qquad\qquad [2.10]$$

The electrostatics interaction is described in the function of atomic charges, which equation is expressed as the Coulomb potential;

$$E_{electrostatic} = \sum_{\substack{non-bonded \\ pair}} \frac{q_i q_j}{r_{ij}} \qquad\qquad [2.11]$$

where   $q_i, q_j$   is the charges of atom $i, j$,

and     $r_{ij}$    is the distance between two atoms.

## 2.3    Molecular Dynamics Simulations

### 2.3.1   Background

Molecular dynamics (MD) simulation is the method that used to describe the time-dependent behavior of the system by solving Newton's equations of motion and allowing the structural fluctuations. It is widely used to calculate the properties of the systems as the kinetic and thermodynamic information by concerning the motions of individual particles as a function of times. Molecular dynamics simulations are the one of an effective means used for exploring conformational space, especially for molecules containing hundreds of rotatable bonds.

### 2.3.2 Newton's Law

Since molecular dynamics simulations are the approaches which aim to reproduce the time-dependent motional behavior of a molecule, the Newton's second law is solved and the interaction of the atoms in the molecule is assumed by employing the force field. To treat this technique, the motional equation is given by

$$\vec{F}_i = m_i \vec{a}_i = m_i \frac{d\vec{v}_i}{dt} = m_i \frac{d^2 \vec{r}_i}{dt^2} \qquad [2.12]$$

where  $\vec{F}_i$   is the force which acted on the atom $i$ at time $t$,

   $m_i$   is the mass of the atom $i$,

   $\vec{v}_i$   is the velocity of the atom $i$,

   $\vec{a}_i$   is the acceleration of the atom $i$.

The force, $\vec{F}_i$, can also be expressed as the gradient of the potential energy.

$$\vec{F}_i = -\nabla V_i(\vec{R}) = \frac{dV}{d\vec{r}_i} \qquad [2.13]$$

where  $V_i(\vec{R})$  is the potential energy of the system.

The combining of equations [2.12] and [2.13] is

$$-\frac{dV}{d\vec{r}_i} = m_i \frac{d^2 \vec{r}_i}{dt^2} . \qquad [2.14]$$

Therefore the potential energy of changing in the atom position can be related to the Newton's equation of motion as a function of time.

According to equation [2.12], the acceleration is

$$\bar{a}_i = \frac{d\bar{v}_i}{dt} \qquad [2.15]$$

The integration is used to calculate the velocity,

$$\bar{v}_i = \bar{a}_i t + v_0 \qquad [2.16]$$

and

$$\bar{v}_i = \frac{d\bar{r}_i}{dt} \qquad [2.17]$$

$$\bar{r}_i = \bar{v}_i t + r_0 \qquad [2.18]$$

thus,

$$\bar{r}_i = \bar{a}_i t^2 + v_0 t + r_0 \qquad [2.19]$$

Based on the initial atom coordinates of the system, new positions and velocities on the atoms can be calculated at time $t$ and the atoms will be moved to these new positions. As a result of this, a new conformation is created. The cycle will then be repeated for a predefined number of time steps. The collection of energetically accessible conformations produced by this procedure is called an *ensemble*. The steps in a molecular dynamics simulation of an equilibrium system are as follows:

1. Choose initial positions for the atoms. For a molecule this is whatever geometry is available, not necessarily an optimized geometry.

2. Choose an initial set of atom velocities. These are usually chosen to obey a Boltzmann distribution for some temperature, then normalized so that the net momentum for the entire system is zero.

3. Compute the momentum of each atom from its velocity and mass.

4. Compute the forces on each atom from the energy expression. This is usually a molecular mechanics force field designed to be used in dynamical simulations.

5. Compute new positions for the atoms a short time later, called the time step. This is a numerical integration of Newton's equations of motion using the information obtained in the previous steps.

6. Compute new velocities and accelerations for the atoms.

7. Repeat steps 3 through 6.

8. Repeat this iteration long enough for the system to reach equilibrium. In this case, equilibrium is not the lowest energy configuration; it is a configuration that is reasonable for the system with the given amount of energy.

9. Once the system has reached equilibrium, begin saving the atomic coordinates every few iterations. This information is typically saved every 5 to 25 iterations. This list of coordinates over time is called a trajectory.

10. Continue iterating and saving data until enough data have been collected to give results with the desired accuracy.

11. Analyze the trajectories to obtain information about the system. This might be determined by computing radial distribution functions, diffusion coefficients, vibrational motions, or any other property computable from this information.

The application of Newton's equations of motion is uniform in all different available molecular dynamics approaches, but they differ in the employed integration algorithms.

In the application of molecular dynamics to search conformational space it is a common strategy to select conformations at regular time intervals and minimize them to the associated local minimum. This procedure has been used in several conformational analysis studies on small molecules, including ring systems.

Unlike quantum mechanical approaches the electrons and nuclei of the atoms are not explicitly included in the calculations. Molecular mechanics considers the atomic composition of a molecule to be a collection of masses interacting with each other via harmonic forces. As a result of this simplification molecular mechanics is a relatively fast computational method practicable for small molecules as well as for larger molecules and even oligomolecular systems.

### 2.3.3　Periodic Boundary
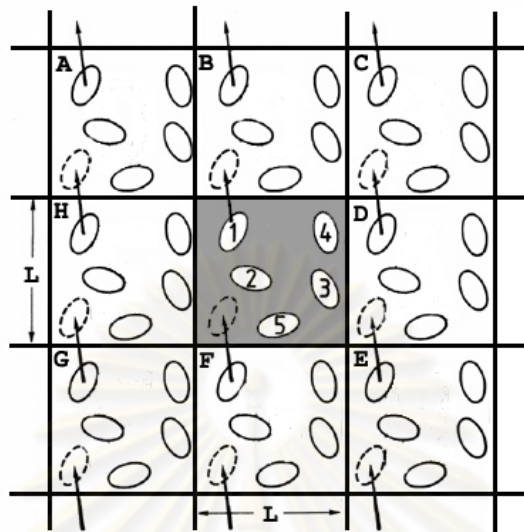


**Figure 2.4** The periodic boundary condition.

In order to model a macroscopic system in term of a finite simulation, the duplication of the system periodically in all directions is employed. In Fig. 2.4, the cubic lattice is used for replication of the central cubic box. The atoms in the periodic boundary box are simply image of the atoms in the simulated box. When a particle moves out of the simulation box, an image particle moves into the simulation box to represent that particle. The calculation of interactions within the cutoff range includes both real and image neighbors.

### 2.3.4　Cut off function

The computational time for calculate the force field energy is in order $n^2$. To reduce the simulation time can be achieved by truncating the van der Waals potential at some distance. To avoid the calculation of distances between all pair of atoms, the contribution is neglected when the distance is larger than a cut-off distance. Under the cut-off situation the van der Waals energy is set to zero but not employed in the Coulomb interaction.

### 2.3.5 Velocity Integrator Model

In order to integrate the equations of motion, the numerical algorithms have been employed to approximate as a Taylor series expansion. It is used to approximate the positions, velocities and accelerations. In this work, the Verlet algorithm was applied which is designed to allow velocities to be calculated at each step.

The basic idea of Verlet algorithm is the combining between the time forward and backward third-order Taylor expansions for the position $\vec{r}(t)$.

$$\vec{r}(t + \Delta t) = \vec{r}(t) + \vec{v}(t)\Delta t + \frac{1}{2}\vec{a}(t)\Delta t^2 + \ldots \qquad [2.20]$$

$$\vec{r}(t - \Delta t) = \vec{r}(t) - \vec{v}(t)\Delta t + \frac{1}{2}\vec{a}(t)\Delta t^2 - \ldots \qquad [2.21]$$

When combine the equations [2.20] and [2.21], the basic form of Verlet algorithm is shown in equation [2.22]

$$\vec{r}(t + \Delta t) = 2\vec{r}(t) - \vec{r}(t - \Delta t) + \vec{a}(t)\Delta t^2 \qquad [2.22]$$

# CHAPTER III

# CALCULATIONS DETAILS

## 3.1    Preparation of Carbon Nanotube Structure

The zigzag (18,0) single wall carbon nanotube (SWCNT) with a diameter of 14 Å is used as the gemcitabine drug carrier. The 20 Å and 34 Å SWCNT structures were generated from the Nanotube Modeler package [50] with chiral vectors $m = 18$, $n = 0$ (Fig. 3.1a). The 36 hydrogen atoms were added at both ends of the SWCNT to complete its structure. The two functional groups, –COOH and –OH, were added on the outer surface of the tube with the length of 20 Å (Figs. 3.1b and 3.1c). For the 34 Å SWCNT, the surface was modified by the carboxyl (-COOH) and hydroxyl (-OH) groups with the density of $1.59/nm^2$ [42]. In total, the 24 functional groups were modified at the exterior surface of the SWCNT (Figs. 3.2b and 3.2c).
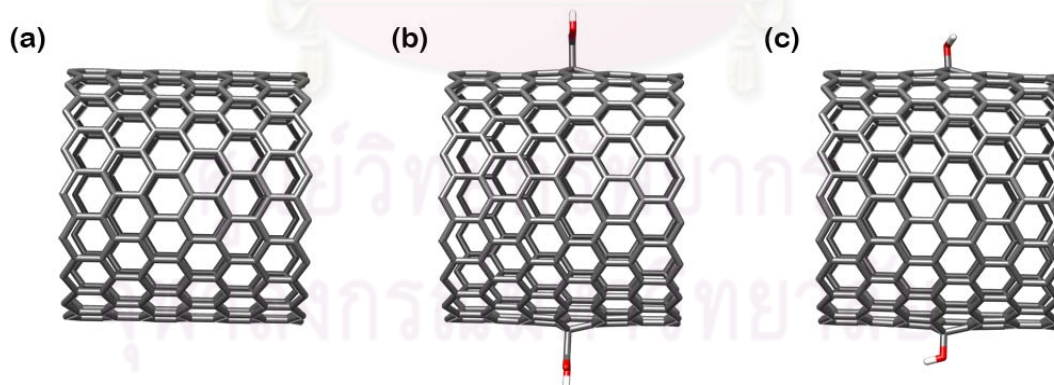


**Figure 3.1** The input structures of (a) (18,0) single-walled carbon nanotube (CNT), the SWCNTs which are modified at the surface with (b) –COOH and (c) –OH groups in quantum chemical calculations.
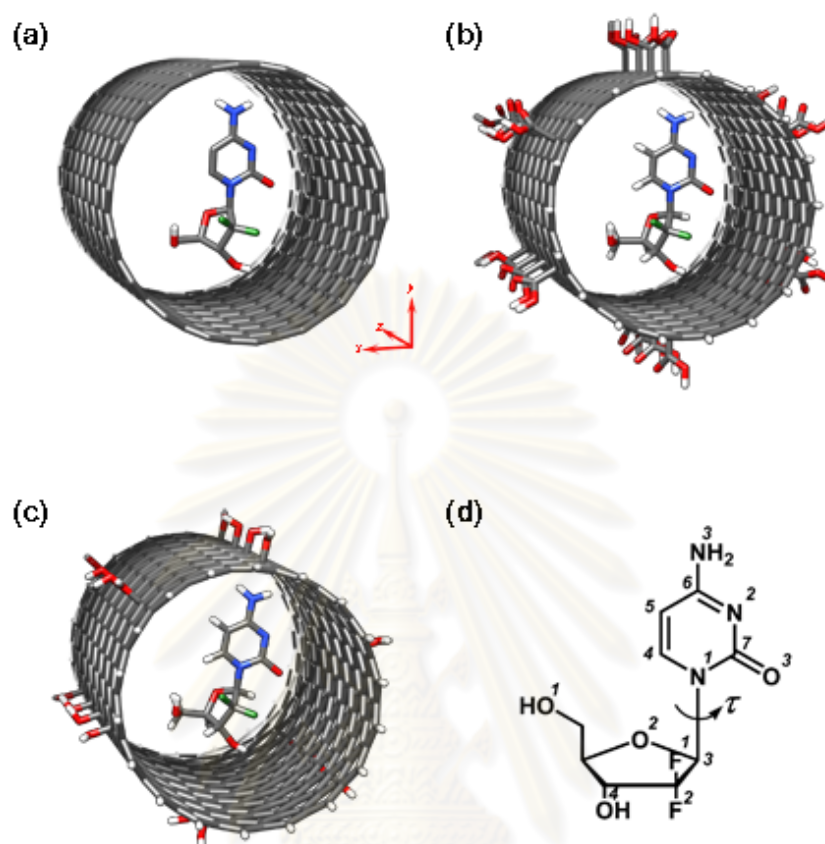
**Figure 3.2** The starting structures of gemcitabine binding to three different SWCNTs: (a) pristine CNT and the modified SWCNTs with (b) –COOH and (c) –OH groups, where atomic labels and torsion angle ($\tau$) were also defined.

## 3.2 Preparation of Gemcitabine Structure

To construct the gemcitabine-SWCNT complexes, the anti-cancer drug extracted from the crystal structure of the human deoxycytidine kinase with gemcitabine bound (Protein Data Bank (PDB), code 2NO0) were added by hydrogen atoms to compete the hybridization of the covalent bonds.

### 3.3 Quantum Chemical Calculations

To find the optimal structures of the SWCNT and its derivatives, the quantum chemical calculations at simi-empirical PM3 method was applied using Gaussian 03 program [51]. The calculated structures were monitored in terms of the bond length, bond angle and the torsion angle of the focused atoms involving the anchored atoms.

### 3.4 Molecular dynamics simulations

To construct the molecular geometry of the gemcitabine-SWCNT complexes, the drug was placed in the middle of the pore of a pristine and two functionalized CNTs (Fig. 3.2). Hydrogen atoms were added to the drug molecule and tube at both ends using the LEaP module in the AMBER 9 software package [52].

The parameters of SWCNT were taken from AMBER99 force field [53] in atom type CA, which were designed for aromatic carbon atoms while the atomic charges and parameters of gemcitabine were obtained as follows. Firstly, the optimization on the drug structure was performed using Gaussian03 program at Hartree-Fock (HF) level of theory using the 6-31G* basis set. Electrostatic potentials (ESP) surrounding the compound were then computed at the same basis set and level of theory. The RESP charge-fitting procedure was applied and the partial charges of equivalent atoms were fitted into the identical value using the RESP module of AMBER 9. Parameters of gemcitabine were created by considering parameters of cytosine and ribose where the parameters involving the fluorine atom were obtained from the Generalized AMBER Force Field (GAFF) [53]. The atomic charges of carboxylic and hydroxyl groups were obtained from the RESP

charges of the aspartic acid and threonine residues, respectively. These partial charges are summarized in Table 3.1.

**Table 3.1** The partial charges for the –COOH and –OH groups modified on the outer surface of carbon nanotube.

| | Site | $q_i$ |
|---|---|---|
| Carbon Nanotube | | |
| | C | 0.0 |
| –COOH | | |
| | C[a] | 0.08 |
| | C | 0.68 |
| | =O | -0.59 |
| | O | -0.67 |
| | H | 0.50 |
| –OH | | |
| | C[a] | 0.22 |
| | O | -0.72 |
| | H | 0.50 |

[a]Anchored carbon on the nanotube

The drug in free state and the drug-SWCNT complex were solvated with a SPC/E [54] octagonal box over 12 Å from the system surface. Any water molecules of which the oxygen atoms were sterically overlapped with the heavy atoms of the drug and the SWCNT molecules were removed. Here, the systems of free drug and its complex in the pristine, –COOH and –OH functionalised SWCNT contain 3296, 14627, 13655 and

14192 atoms in total, respectively. The simulations were performed using the SANDER module of AMBER 9 program package with *NPT* ensemble at 1 atm and the time step of 2 fs. The SHAKE algorithm [55] was applied to all bonds involving the hydrogen atoms to constraint their motions. The periodic boundary conditions were applied and the cutoff function was set at 12 Å for nonbonded interactions and particle mesh Ewald method [56-57]. The whole system was heated from 100 K to 300 K for 25 ps and equilibrated at 300 K for 600 ps. Then, the production stage was performed for 10 ns in which the structural coordinates were saved every 1 ps for analysis.

# CHAPTER IV

# RESULTS AND DISCUSSION

## 4.1 Optimized Structures of SWCNTs Based on Quantum Chemical Calculations

The bond lengths, bond angles and improper torsion angle are measured from the optimized PM3 structures of the three different systems, a pristine and two functionalized SWCNTs. The B1-B3 bond lengths from the anchored carbon atom, $C^a$, to its connected carbon atoms, $C^1$, $C^2$, and $C^3$, as well as their involving angles are defined in Fig. 4.1 also summarized in Table 2. It can be seen that all bonds are lengthened by 0.1 Å from the pristine CNT (1.4 Å) to the functionalized CNT systems (1.5 Å). The two functional modifications also affect to all bond angles, A1-A3, by a reduction of 8-10 degree in respect to those of the pristine CNT. This consequently leads to a loss of the planarity of the tube surface indicated by an increase of the improper torsion angle, $C^a$-$C^1$-$C^2$-$C^3$, from 5.8 degree in the pristine system to 32 degree in the functionalized systems. The calculated results were, then, compared to those obtained from the molecular dynamics simulations.
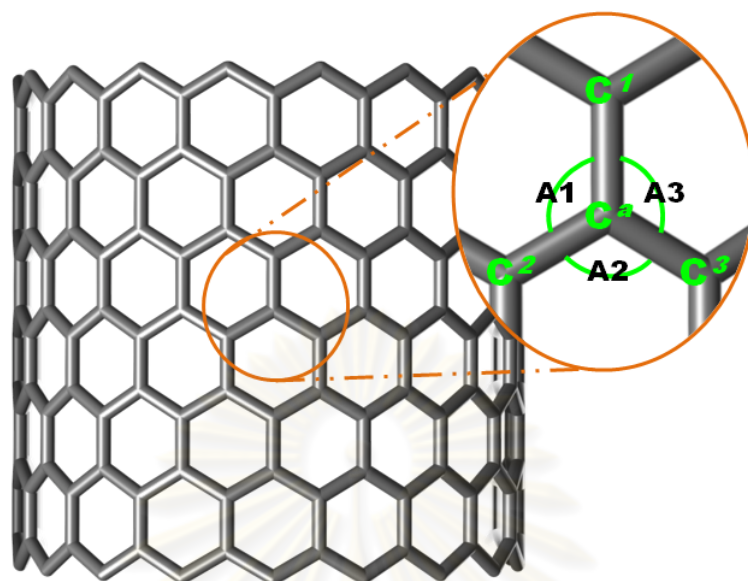
**Figure 4.1** Systematic view of the functionalized SWCNT where the anchored carbon atom, $C^a$, and its adjacent atoms are closed up. The bond angles are also defined.

**Table 4.1** The structural properties of three different systems calculated by the PM3 method.

| | Bond length (Å) | | | Bond angle (degree) | | | Torsion (degree) $C^a$-$C^1$-$C^2$-$C^3$ |
|---|---|---|---|---|---|---|---|
| | **B1** | **B2** | **B3** | **A1** | **A2** | **A3** | |
| **SWCNT** | 1.421 | 1.420 | 1.420 | 120.0 | 119.2 | 120.0 | 5.8 |
| **SWCNT-COOH** | 1.508 | 1.515 | 1.516 | 112.1 | 109.7 | 112.1 | 32.8 |
| **SWCNT-OH** | 1.515 | 1.523 | 1.519 | 111.8 | 110.1 | 112.0 | 32.6 |

## 4.2 Molecular Dynamics Simulations

The molecular dynamics simulations are performed to calculate the structural properties and the dynamical properties of the drug filling inside three types of the 34 Å SWCNT: a pristine and two functionalized SWCNTs by adding –COOH and –OH groups on the outer surface.

In terms of molecular geometries, the MD simulation lead to the average bond lengths of the pristine SWCNT, SWCNT–COOH and SWCNT–OH of 1.420 Å, 1.550 Å and 1.510 Å with the corresponding bond angles of 119.5°, 110.4° and 110.2°. These agree well with those found using quantum chemical calculations shown in Table 4.1.

### 4.2.1. The pristine SWCNT bound state



**Figure 4.2** The structure of the (18,0) single-walled carbon nanotube (SWCNT) complexed with the gemcitabine drug where atomic labels and torsion angle ($\tau$) were also defined. The origin of the Cartesian coordinate for the complex was centered at the center of gravity ($Cg$) of the SWCNT.

### 4.2.1.1. Existing of the Drug-SWCNT complex

To examine the feasibility of the use of the SWCNT as nano-container in drug delivery application, the existing of the drug-SWCNT complex was monitored in terms of the center of gravity ($Cg$) of drug molecule distributed inside the tube. Along the SWCNT's axis ($z$-axis defined in Fig. 4.2), displacement $Cg$ of drug, $d(Cg)$, as a function of simulation time was shown in horizontal plot in Fig. 4.3a, while the probability of finding the $Cg$ of drug molecule, $P(Cg)$, was illustrated in vertical plot in the same figure. To monitor the movement of drug in the direction perpendicular to the SWCNT surface, the averaged projection of the $P(Cg)$ to the tube $x$- and $y$-axis (defined in Fig. 4.2) were also calculated and given in Fig. 4.3b.

In Fig. 4.3a, the $d(Cg)$ in the horizontal plot shows that at the initial step ($t = 0$), drug molecule was located at the center of the SWCNT ($Cg = 0$). Regular movement of the drug molecule from one end ($d(Cg) = -12.5$ Å) to the other ($d(Cg) = +12.5$ Å) of the 34 Å SWCNT can be clearly seen. In addition, the drug has never visited to the inner surface at the distance of $< 4.5$ Å from the two ends of the tube, $i.e.$, drug molecule is able to move freely and remain only inside its container. This is surely due to the repulsion with the hydrogen atoms at both ends. The observed event was well supported by the $P(Cg)$ plot (the vertical plot in Fig. 4.3a) in which the probability was found to increase exponentially as a function of the distance from the two ends of the SWCNT. Note that the symmetric distribution of the $P(Cg)$ plot is expected if the sampling size is large enough, the long enough simulation time.

In the same manner, the probability of finding $Cg$ of drug molecule in the direction perpendicular to the tube surface ($x$- and $y$-axis) showed only one distinct peak at 2.3 Å from the origin of the coordinate system indicating that drug molecule does not prefer to

move at the center along the tube *z*-axis but the favorite motion is ~ 4.7 Å away from the inner surface instead. It is therefore the aromatic stacking interaction between drug and the SWCNT surface was formed (discussed in the next section). Taking into account all the above mobility data, the drug molecule was found to coordinate inside the SWCNT, an existing of the drug-SWCNT complex, during the whole simulation time of 10 ns. Therefore, the SWCNT terminated by the hydrogen atoms is supposed to be used as drug container in the drug delivery system.
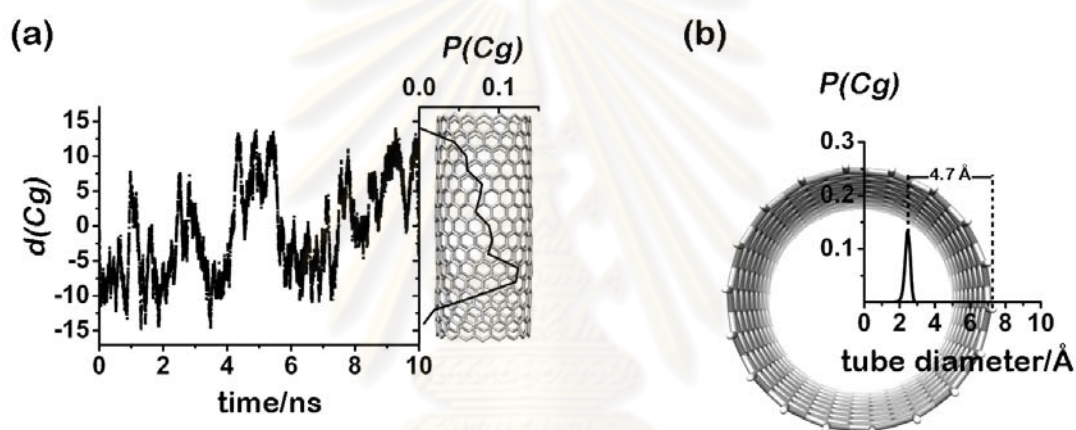


**Figure 4.3** (a) Displacement of center of gravity of drug molecule, *d(Cg)*, as a function of simulation time (horizontal plot) and probability of finding the *Cg* of drug molecule (vertical plot), *P(Cg),* projected onto the SWCNT *z*-axis; (b) *P(Cg)* in the directions perpendicular to the SWCNT surface (*x*- and *y*-axis).

### 4.2.1.2. Conformation of drug in free and complex forms
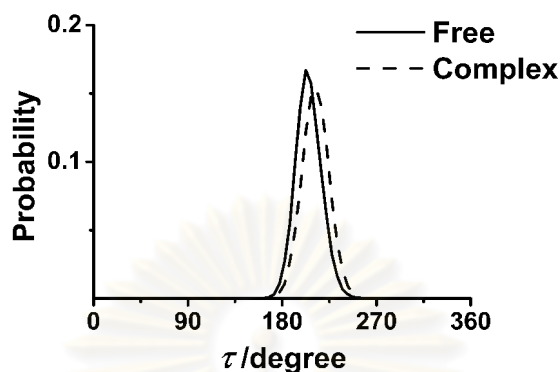


**Figure 4.4** Distribution of the $C^7$-$N^1$-$C^3$-$O^2$ torsion angle, $\tau$ (see Fig. 4.2 for its definition and atomic labels), of the gemcitabine in free (solid line) and complex (dash line) forms.

To examine the conformation as well as flexibility of drug molecule in free state and inside the SWCNT, the relative orientation of the ribose ring (five-membered ring) and cytosine ring (six-membered ring) defined as the $C^7$-$N^1$-$C^3$-$O^2$ torsion angle *($\tau$)* in Fig. 4.2, was calculated and compared in Fig. 4.4. No significant difference was found in terms of drug conformation in these two states in which the most probable torsion angle of the free and complex forms was observed at 210° and 215°, respectively. Note that the distribution plot showed a broad peak covering the range of 80°, precisely from 170° to 250° for the free form and from 180° to 260° for the complex. This conferred that the drug molecule is rather flexible and insensitive to the environment, in aqueous solution and inside the SWCNT. Therefore, utilizing CNT as the gemcitabine carrier does not affect the conformation of drug itself.
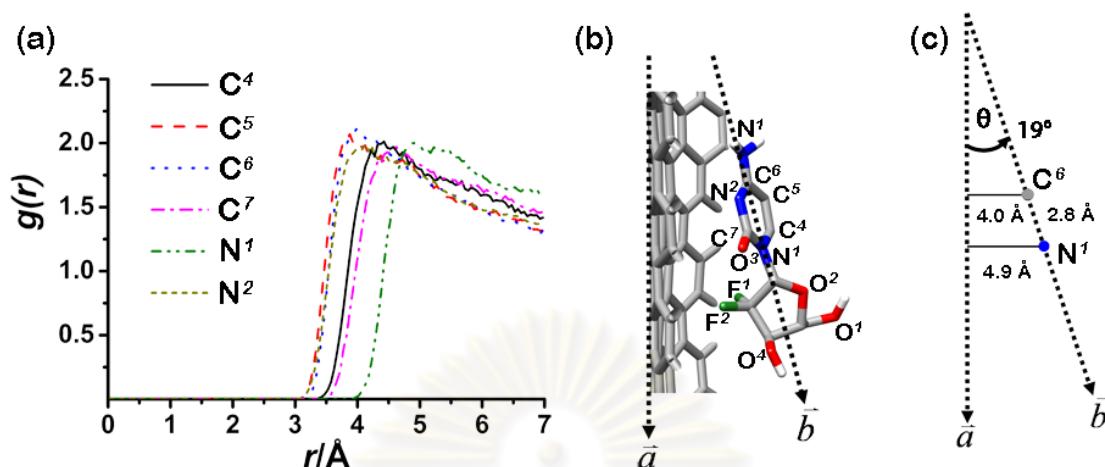
**Figure 4.5** (a) RDFs centered at the atoms in the cytosine (six-membered) ring of the gemcitabine drug ($C^4$-$C^7$, $N^1$ and $N^2$) to carbon atoms of the SWCNT; (b) Schematic representation of the drug-SWCNT complex where vector $\vec{a}$ lies parallel to the SWCNT surface and vector $\vec{b}$ points from $C^6$ to $N^1$ atoms; (c) Estimated angle between vectors $\vec{a}$ and $\vec{b}$ (see text for details of the related distances).

To understand more details of molecular alignment of drug molecule inside the SWCNT, the atom-atom radial distribution functions (RDFs), expressed as $g_{ij}(r)$ −the probability of finding a particle of type $j$ in a sphere of radius, $r$, around a particle of type $i$− were calculated. Interest is focused to the cytosine (six-membered) ring whose π-aromatic system was expected to preferably deposited and directly interact to the inner surface of the SWCNT. Therefore, in this study $i$ denotes the backbone atoms of the cytosine ring ($C^4$-$C^7$, $N^1$ and $N^2$) and $j$ represents the carbon atoms of the SWCNT. The calculated RDFs were summarized in Fig. 4.5a. Schematic representation of the drug-SWCNT complex where vector $\vec{a}$ lies parallel to the SWCNT surface and vector $\vec{b}$ points from $C^6$ to $N^1$ atoms was in Fig. 4.5b.

In Fig. 4.5a, the six RDF plots can be classified into 3 sets; $\{C^5, C^6, N^2\}$, $\{C^4, C^7\}$ and $\{N^1\}$ in which their $g(r)$s were detected for the first time ($g(r) \neq 0$) at 3.0 Å, 3.4 Å and 3.8 Å with the maxima at $\sim$ 4.0 Å, $\sim$ 4.5 Å and 4.9 Å, respectively. Using the most probable distances from the $C^6$ ($\sim$ 4.0 Å maximum of the $C^6$-C RDF) and $N^2$ ($\sim$ 4.9 Å maximum of the $N^2$-C RDF) atoms to the SWCNT surface, and the $N^2$-$C^6$ distance (2.8 Å), the angle between the vectors $\bar{a}$ and $\bar{b}$ can be estimated (Fig. 4.5c). The obtained value of $19^o$ indicates the tilted angle representing the configuration of $\pi$-$\pi$ stacking interaction between the cytosine ring of the gemcitabine and the inner surface of the SWCNT. This interaction is supposed to be the main reason why the preferential mobility of drug molecule along the molecular $z$-axis of the SWCNT takes place at $\sim$ 4.7 Å far from the surface of the SWCNT (Fig. 4.3b).

### 4.2.1.3. Solvation of the drug in free and complex forms

The solvation of ligand was monitored by the atom-atom radial distribution functions. Here, the RDFs to oxygen atom of water around the heteroatom in drug molecule were evaluated and plotted in Fig. 4.6 for the drug molecule in free and complex forms. The corresponding running integration numbers, $n(r)$, were also calculated and shown. The first shell coordination number, $CN$, around the atoms of drug (defined in Fig. 4.2) in both systems obtained from the integration up to the first minimum of the RDF were summarized in Table 4.2.

The plots for both systems showed almost sharp first peaks indicating strong solvation, high water accessibility, to the central atoms of the drug molecule. Remarkably changes were found on the RDFs of the fluorine atoms, especially $F^2$. In the complex form, the first shell RDF of $F^1$ atom displayed the lower intensity while that of $F^2$ atom

was almost disappear *i.e.,* water molecules cannot feasibly access to those two atoms. This is due to the fact that these atoms in the complex form were turned to approach to the SWCNT surface (see Fig. 4.5b). Moreover, a considerable difference was also observed on the height of the *g(r)* in the region between the first and the second peaks of almost all RDFs which denotes a feasibility of water exchange between the two shells. These values for the drug in free (Figs. 4.6a, 4.6b and 4.6c) were noticeably higher than those in the complex forms. This implies that water molecules in the first hydration shell bind stronger to the drug atoms in the complex form than those in the free form. The reason for this finding can be because of the collaborative effect due to the aromatic stacking interactions with the inner surface of the SWCNT (see also Fig. 4.5b) as discussed above.
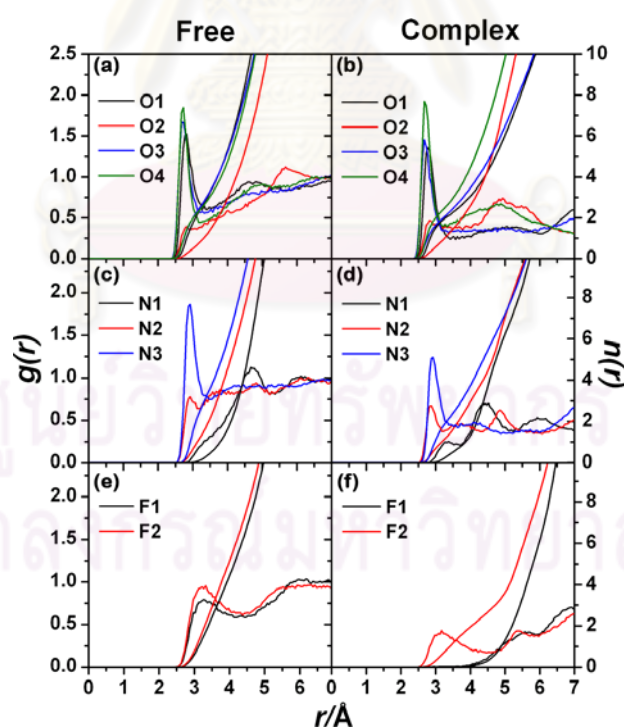


**Figure 4.6** Radial distribution functions, *g(r)*, centered on the inhibitor atoms (see Fig. 4.2 for definitions) to oxygen atoms of modeled water of the free and complex systems, including the running integration number up, *n(r)*.

**Table 4.2** First shell coordination number, *CN*, around the atoms of drug (defined in Fig. 4.2) in free and complex forms, obtained from the integration up to the first minimum of the atom-atom RDF, *g(r)*, shown in Fig. 4.6.

| Atom | CN | |
|---|---|---|
| | free | complex |
| $O^1$ | 2.5 | 2.4 |
| $O^2$ | 0.7 | 0.6 |
| $O^3$ | 3.0 | 2.3 |
| $O^4$ | 2.6 | 2.5 |
| $N^1$ | - | 0.8 |
| $N^2$ | 1.5 | 1.0 |
| $N^3$ | 3.8 | 3.3 |
| $F^1$ | 4.7 | - |
| $F^2$ | 6.5 | 2.3 |

Changes of the first shell coordination numbers of drug molecule, in comparison between its free and complex states (Table 4.2) can be classified into 3 sets; notably decrease $\{F^1, F^2\}$, slightly decrease $\{O^3, N^1, N^2, N^3\}$ and almost the same $\{O^1, O^2, O^4\}$. This is a consequence of the conformational changes of the drug molecule where the 3 sets of atoms in the complex form were located in the following configurations relative to the SWCNT surface (Fig. 4.5b); $\{F^1, F^2\}$ was tabbed between the SWCNT inner surface and the five-membered ring (almost no space is available for the solvent); $\{O^3, N^1, N^2, N^3\}$ was positioned in the plane of the six-membered ring that coordinated in the stacked conformation to the SWCNT surface (only half of the space around the atoms can be solvated); $\{O^1, O^2, O^4\}$ was tilted to point away from the SWCNT surface (the atoms in the complex were fully solvated as in free form).

### 4.2.2. The functional systems

The main concept in functionalization of the SWCNTs in drug delivery system is to increase their solubility in the body liquid as well as to decrease their toxicity. In this study, the SWCNT–COOH and SWCNT–OH were chosen. Therefore, the structural and dynamic properties and the solvation of the drug molecule inside the pristine SWCNT and the two functionalized SWCNT were compared in Figs. 4.7-4.10.

In Fig. 4.7 (vertical), probability of finding the center of mass of drug molecule, *P(Cg)*, along the *z*-axis shows preferential positions (peaks) at the functional –COOH (Fig. 4.7c) and –OH (Fig. 4.7e) groups which this event does not show in the pristine SWCNT complex. In addition, no different was focused in term of drug displacement perpendicular to the SWCNT surface (*x-y* axes) of the three complexes.

Considering changes of drug conformation inside the three complexes were compared in Fig. 8, no significant was found in terms of the peak positions (215 °, 202° and 202° for the pristine SWCNT, SWCNT–COOH and SWCNT–OH) indicating relative orientation of the the ribose and the cytosine-based ring of the drug. Interesting, the functionalized SWCNT leads to a less flexibility of drug molecule thus that in free form (solid black for free drug in aqueous solution) and inside the pristine SWCNT. This was indicated by a narrower of the peaks for the functionalized (SWCNT–COOH and SWCNT–OH) SWCNT than those of the other two systems.

In terms of drug's orientation shown by the atom-atom RDFs in Fig. 4.9. The cytosine-based ring of the drug in the three complexes was focused to bind in stacking conformation to the inner surface of the tube. The plots in Fig. 4.9 show that they were found to orient in the same manner, the RDFs and the tilted angles (shown by snapshot in Fig. 4.9b, 4.9d and 4.9f) take place at the same position.

Because of the orientation (Fig. 4.9) of the drug in the three systems are almost same for the drug molecule in the pristine and in the functionalized SWCNTs, no significant different was found on the RDFs of water around the O, N and F atoms of drug molecule (Fig. 4.10). Therefore, the peak were almost shown to take place at the same distance and the same probability. This means that functional –COOH and –OH groups do not affect to the drug solvation.
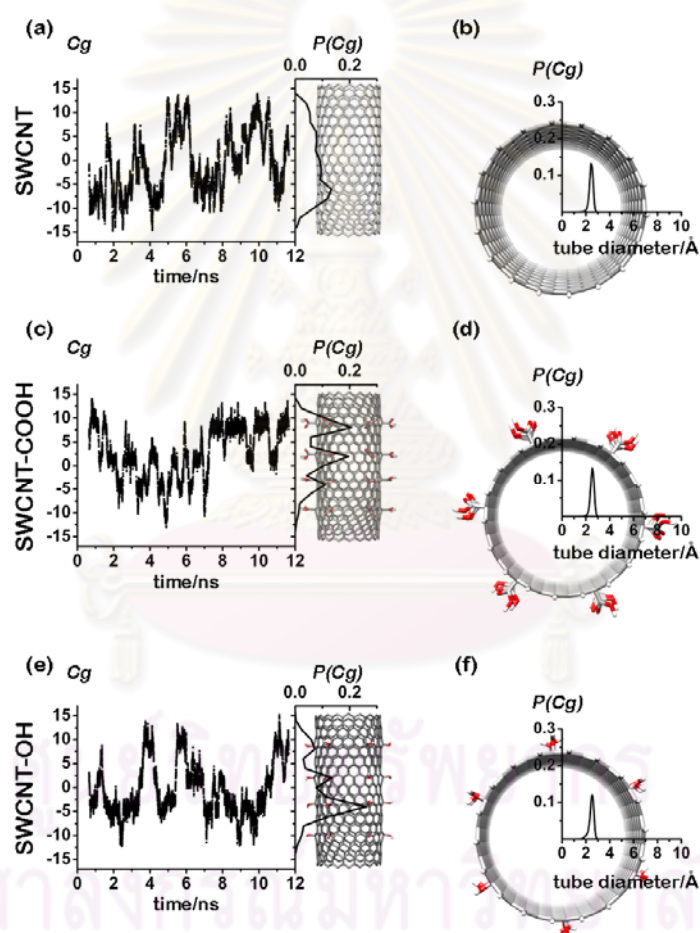


**Figure 4.7** (c-e) Projection of the center of mass of gemcitabine drug onto the *z*-axis of the three complexes sampled during the simulations and the corresponding existence probabilities of drug at the position in the same *z*-axis as well as (d-f) the average probabilities in *x*- and *y*-axes of the SWCNT tube.
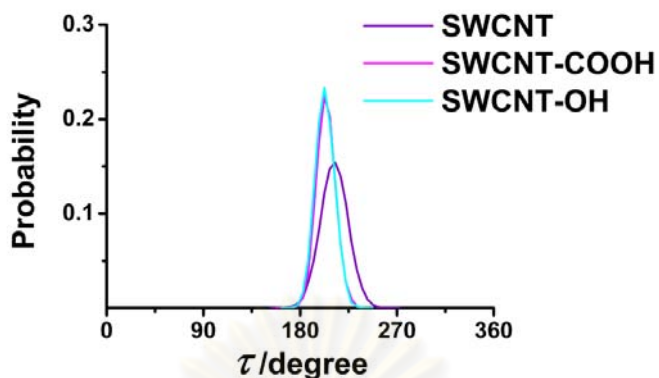
**Figure 4.8** Distribution of the $C^7$-$N^1$-$C^3$-$O^2$ internal torsion ($\tau$) of gemcitabine in bound with SWCNT (purple), SWCNT-COOH (pink) and SWCNT-OH (cyan) states. The atomic label and the location of $\tau$ are also shown.
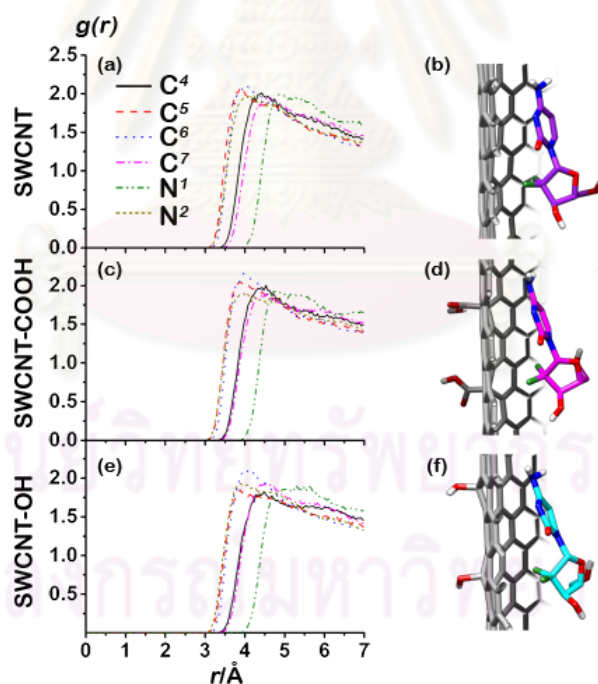


**Figure 4.9** RDFs for C atoms from different atoms in the cytosine-base ring (six-memberred ring) of the gemcitabine drug to the atoms of the three SWCNT complexes.
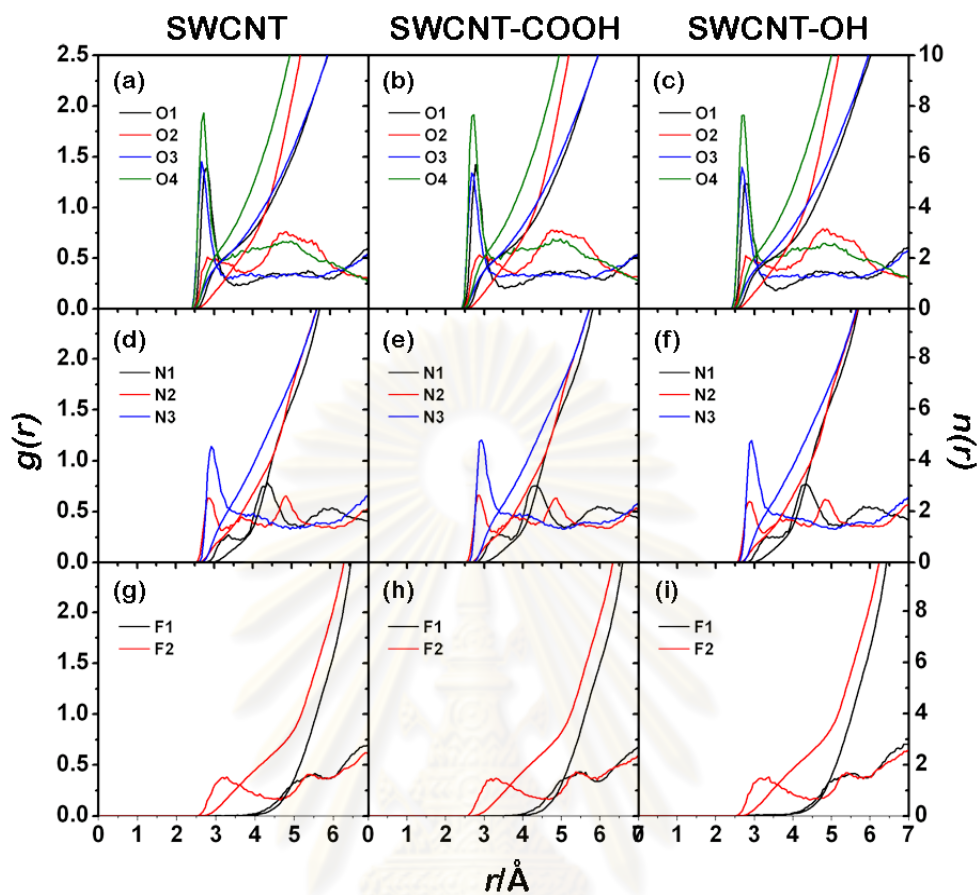
**Figure 4.10** Radial distribution functions, *g(r)*, centered on the inhibitor atoms (see Fig. 4.2 for definitions) to oxygen atoms of modeled water of the free and complexed systems, including the running integration number up, *n(r)*.

# CHAPTER V

# CONCLUSIONS

Two different theoretical approaches, the quantum chemical (QM) calculation and molecular dynamics (MD) simulations, have been applied on the single-walled carbon nanotube (SWCNT), with or without carrying the gemcitabine anticancer drug. At first, the pristine and functionalized SWCNTs with the length of 20 Å were studied by the QM calculation with the simiempirical PM3 method. It was found that the structural properties involving the anchored carbon atom were considerably changed after modification on the outer surface of the tube by –COOH and –OH functional groups. There are bond lengthened by 0.1 Å, angle reduction of 8-10° and increase of improper angle of 27° suggesting the lowered planarity of the tube surface. Furthermore, the PM3 molecular geometries of the pristine and the functionalized SWCNTs are in good agreement with those obtained from the MD results of the gemcitabine-SWCNTs.

To investigate the structural and dynamical properties of using the single walled carbon nanotube (SWCNT) as a gemcitabine drug carrier. The drug filling inside SWCNT was extensively investigated in comparison to the drug in free state. According to the local density distributions of drug projected to the diameter (xy-plane) and the length (z-axis) of SWCNT, the drug was able to simultaneously move from one end to the other of the SWCNT but has never visited to the surface at the distance of < 4.5 Å from two ends of the tube. This translocation is not along the parallel to the tube axis at the center of the tube, but the favorite motion (from the center of mass of the drug) is ~ 4.7 Å

away from the inner surface where the cytosine-based ring of drug was found to bind in stacking conformation to the inner surface of the tube with tilted angle of 19°. This data suggested that the drug molecule is able to move freely and remain only inside the SWCNT container with a formation of the probable aromatic stacking interactions to the inner surface. Although the cytosine-ribose conformation of the drug in free and bound states was relatively similar, the drug solvation was shielded at the $O^2$, $N^1$, and $F^2$ atoms by the collaborative interaction with the inner surface of the tube. The MD simulations were further performed on the two functionalized SWCNTs with –COOH and –OH substituents on the outer surface, however no significant differences in terms of drug conformation, orientation and solvation were observed.

# REFERENCES

[1]    Sumio Iijima. Helical microtubules of graphitic carbon. Nature 354 (1991) :
        56-58.

[2]    Alberto Bianco, Kostas Kostarelos, Charalambos D. Partidos and Maurizio Prato.
        Biomedical    applications    of    functionalised    carbon    nanotubes.
        Chem. Commun. (2005) : 571-577.

[3]    Andrei M Popov, Yurii E Lozovik, Silvana Fiorito, L'Hocine Yahia.
        Biocompatibility  and  applications  of  carbon  nanotubes  in  medical
        nanorobots. Int. J. Nanomed. 2 (2007) : 361-372.

[4]    S.K. Smart, A.I. Cassady, G.Q. Lu, D.J. Martin. The biocompatibility of carbon
        nanotubes. Carbon 44 (2006) : 1034-1047.

[5]    Sarbajit Benerjee, Tirandai Hemraj-Benny, and Stanislaus S. Wong. Covalent
        Surface  Chemistry  of  Single-Wall  Carbon  Nanotubes.  Adv.  Mater.
        1 (2005) : 17-29.

[6]    Giorgia Pastorin, Wei Wu, Sébastien Wieckowski, Jean-Paul Briand, Kostas
        Kostarelos, Maurizio Prato and Alberto Bianco. Double functionalisation
        of carbon nanotubes for multimodal drug delivery. Chem. Commun.
        (2006): 1182-1184.

[7]    Cédric  Klumpp,  Kostas  Kostarelos,  Maurizio  Prato,  Alberto  Bianco.
        Functionalized carbon nanotubes as emerging nanovectors for the delivery
        of therapeutics. BBA 1758 (2006) : 404-412.

[8]    Kostas Kostarelos, Lara Lacerda, Giorgia Pastorin, Wei Wu, Sébastien
        Wieckowski,  Jacqueline  Luangsivilay,  Sylvie  Godefroy,  Davide

Pantarotto, Jean-Paul Briand, Sylviane Muller, Maurizio Prato and Alberto Bianco. Cellular uptake of functionalized carbon nanotubes is independent of functional gropu and cell type. <u>Nat. Nanotechnol.</u> 2 (2007) : 108-113.

[9]     Vittoria Raffa, Gianni Ciofani, Stephanos Nitodas, Theodoros Karachalios, Delfo D Alessandro, Matilde Masini, Alfred Cuschieri. Can the properties of carbon nanotubes influence their internalization by living cell? <u>Carbon</u> 46 (2008) : 1600-1610.

[10]    Xiaoke Zhang, Lingjie Meng, Qinghua Lu, Zhaofu Fei, Paul J. Dyson. Targeted delivery and controlled release of doxorubicin to cancer cells using modified single wall carbon nanotubes. <u>Biomaterials</u> 30 (2009) : 6041-6047.

[11]    Feazell RP, Nakayama-Ratchford N, Dai H, Lippard SJ. Soluble Single-Walled Carbon Nanotubes as Longboat Delivery Systems for Platinum(IV) Anticancer Drug Design. <u>J. Am. Chem. Soc.</u> 129 (2007) : 8438–8439.

[12]    Liu Z, Sun X, Nakayama N, Dai H. Supramolecular Chemistry on Water-Soluble Carbon Nanotubes for Drug Loading and Delivery. <u>ACS Nano</u> 1 (2007) : 50–56.

[13]    Bianco A, Kostarelos K, Prato M. Applications of carbon nanotubes in drug delivery. <u>Curr. Opin. Chem. Bio.</u> 9 (2005) : 674–679.

[14]    C. Srinivasan. Carbon nanotubes in cancer therapy. <u>Curr. Sci.</u> 94 (2008) : 300-301.

[15]    Zhuang Liu, Kai Chen, Corrine Davis, Sarah Sherlock, Qizhen Cao, Xiaoyuan Chen, and Hongjie Dai. Drug delivery with carbon nanotubes for in vivo cancer treatment. <u>Cancer Res</u> 68 (2008) : 6652-6660.

[16]  Bianco A, Prato M: Can carbon nanotubes be considered useful tools for biological applications? Adv. Mater. 15 (2003) : 1765-1768.

[17]  Salvador-Morales C, Flahaut E, Sim E, Sloan J, Green MLH, Sim RB. Complement activation and protein adsorption by carbon nanotubes. Mol. Immunol. 43 (2006) : 193-201.

[18]  Pantarotto D, Partidos CD, Graff R, Hoebeke J, Briand JP, PratoM, Bianco A. Synthesis, Structural characterization and immunological properties of carbon nanotubes functionalized with peptides. J. Am. Chem. Soc. 125 (2003) : 6160-6164.

[19]  Pantarotto D, Partidos CD, Hoebeke J, Brown F, Kramer E, Briand JP, Muller S, Prato M, Bianco A. Immunization with peptide-functionalized carbon nanotubes enhances virusspecific neutralizing antibody responses. Chem. Biol. 10 (2003) : 961-966.

[20]  Pantarotto D, Briand JP, Prato M, Bianco A. Translocation of bioactive peptides across cell membranes by carbon nanotubes. Chem. Commun. (2004) : 16–17.

[21]  Shi Kam NW, Dai H. Carbon Nanotubes as Intracellular Protein Transporters: Generality and Biological Functionality. J. Am. Chem. Soc. 127 (2005) : 6021-6026.

[22]  Kazuhiro Yanagi, Yasumitsu Miyata, and Hiromichi Kataura. Highly Stabilized β-Carotene in Carbon Nanotubes. Adv. Mater. 18 (2006) : 437-441.

[23]  Kazuhiro Yanagi, Konstantin Iakoubovskii, Said Kazaoui, Nobutsugu Minami, Yutaka Maniwa, Yasumitsu Miyata, and Hiromichi Kataura. Light-

harvesting function of β-carotene inside carbon nanotubes. Phys. Rev. B 74 (2006) : 155420.

[24]   Liu Y, Wu DC, Zhang WD, et al. Polyethylenimine-grafted multiwalled carbon nanotubes for secure noncovalent immobilization and efficient delivery of DNA. Angew. Chem. Int. Ed. 44 (2005) : 4782.

[25]   Kam NWS, Liu Z, Dai H. Functionalization of carbon nanotubes via cleavable disulfide bonds for efficient intracellular delivery of siRNA and potent gene silencing. J. Am. Chem. Soc. 36 (2005) : 12492–12493.

[26]   Liu Z, Winters M, Holodniy M, Dai H. siRNA delivery into human T cells and primary cells with carbon-nanotube transporters. Angew. Chem. Int. Ed. 46 (2007) : 2023–2027.

[27]   Maurizio Prato, Kostas Kostarelos, and Alberto Bianco. Functionalized Carbon Nanotubes in Drug Design and Discovery. Acc. Chem. Res. 41 (2008) : 60-68.

[28]   Vicki L Colvin. The potential environmental impact of engineered nanomaterials. Nat. Biotech. 21 (2003) : 1166-1170.

[29]   Christie M. Sayes, Feng Liang, Jared L. Hudson, Joe Mendez, Wenhua Guo, Jonathan M. Beach, Valerie C. Moore, Condell D. Doyle, Jennifer L. West, W. Edward Billups, Kelvin D. Ausman, Vicki L. Colvin. Functionalization density dependence of single-walled carbon nanotubes cytotoxicity in vitro. Toxicology Letters 161 (2006) : 135-142.

[30]   H. Kuzmany, A. Kukovecz, F. Simon, M. Holzweber, Ch. Kramberger, T. Pichler. Functionalization of carbon nanotubes. Synthetic Metals 141 (2004) : 113-122.

[31]     Jijun Zhao, Hyoungki Park, Jie Han, and Jian Ping Lu. Electronic Properties of Carbon Nanotubes with Covalent Sidewall Functionalization. J. Phys. Chem. B 108 (2004) : 4227-4230.

[32]     Marcos V. Veloso, A.G. Souza Filho, J. Mendes Filho, Solange B. Fagan, R. Mota. *Ab initio* study of covalently functionalized carbon nanotubes. Chem. Phys. Letts. 430 (2006) : 71-74.

[33]     Alessio Alexiadis and Stavros Kassinos. Molecular Simulation of Water in Carbon Nanotubes. Chem. Rev. 108 (2008) : 5014-5034.

[34]     J.H. Walther, R. Jaffe, T. Halicioglu, and P. Koumoutsakos. Carbon Nanotubes in Water: Structural Characteristics and Energetics. J. Phys. Chem. B. 105 (2001) : 9980-9987.

[35]     G. Hummer, J. C. Rasaiah, and J. P. Noworyta. Water conduction through the hydrophobic channel of a carbon nanotube. Nature 414 (2001) : 188-190.

[36]     R. Jay Mashl, Sony Joseph, N. R. Aluru, and Eric Jakobsson. Anomalously Immobilized Water: A New Water Phase Induced by Confinement in Nanotubes. Nano Letts. 3 (2003) : 589-592.

[37]     William H. Noon, Kevin D. Ausman, Richard E. Smalley, Jianpeng Ma. Helical ice-sheets inside carbon nanotubes in the physiological condition. Chem. Phys. Letts. 355 (2002) : 445-448.

[38]     A. Striolo, A. A. Chialvo, K. E. Gubbins, P. T. Cummings. Water in carbon nanotubes: Adsorption isotherms and thermodynamics properties from molecular simulation. J. Chem. Phys. 122 (2005) : 234712.

[39]   Yingchun Liu, Qi Wang, Tao Wu, and Li Zhang. Fluid structure and transport properties of water inside carbon nanotubes. <u>J. Chem. Phys.</u> 123 (2005) : 234701.

[40]   Jun Wang, Yu Zhu, Jian Zhou and Xiao-Hua Lu. Diameter and helicity effects on static properties of water molecules confined in carbon nanotubes. <u>Phys. Chem. Chem. Phys.</u> 6 (2004) : 829-835.

[41]   Boda Huang, Yueyuan Xia, Mingwen Zhao, Feng Li, Xiangdong Liu, Yanju Ji, and Chen Song. Distribution patterns and controllable transport of water inside and outside charged single-walled carbon nanotubes. <u>J. Chem. Phys.</u> 122 (2005) : 084708.

[42]   Jie Zheng, Erin M. Lennon, Heng-Kwong Tsao, Yu-Jane Sheng, Shaoyi Jiang. Transport of a liquid water and methanol mixture through carbon nanotubes under a chemical potential gradient. <u>J. Chem. Phys.</u> 122 (2005) : 214702.

[43]   Liang-Liang Huang, Qing Shao, Ling-Hong Lu, Xiao-Hua Lu, Lu-Zheng Zhang, Jun Wang and Shao-yi Jiang. Helicity and temperature effects on static properties of water confined in modified carbon nanotubes. <u>Phys. Chem. Chem. Phys.</u> 8 (2006) : 3836-3844.

[44]   Liang-Liang Huang, Lu-Zheng Zhang, Qing Shao, Jun Wang, Ling-Hong Lu, Xiao-Hua Lu, Shao-Yi Jiang, and Wen-Feng Shen. Molecular Dynamics Simulation Study of the Structural Characteristics of Water Molecules Confined in Functionalized Carbon Nanotubes. <u>J. Phys. Chem. B</u> 110 (2006) : 25761-25768.

[45]   Yudan Zhu, Mingjie Wei, Qing Shao, Linghong Lu, Xiaohua Lu, and Wengfeng Shen. Molecular Dynamics Study of Pore Inner Wall Modification Effect in Structure of Water Molecules Confined in Single-Walled Carbon Nanotubes. J. Phys. Chem. C 113 (2009) : 882-889.

[46]   Huajian Gao, Yong Kong, Daxiang Cui and Cengiz S. Ozkan. Spontaneous Insertion of DNA Oligonucleotides into Carbon Nanotubes. Nano. Letts. 3 (2003) :   471-473.

[47]   Jie Xie, Qingzhong Xue, Qingbin Zheng, Huijuan Chen. Investigation of the interactions between molecules of β-Carotene, Vitamin A and CNTs by MD simulations. Mat. Letts. 63 (2009) : 319-321.

[48]   Xie, Y. H., Soh, A. K. Investigation of non-covalent association of single-walled carbon nanotube with amylose by molecular dynamics simulation. Mat. Letts. 59 (2005) : 971-975.

[49]   David C. Young. Computational Chemistry A Practical Guide for Applying Techniques to Real-World Problems. : A John Wiley & Sons, Inc., Publication. 2001.

[50]   Nanotube Modeler : JCrystalSoft (http://www.jcrystal.com/products/wincnt/), 2004–2005.

[51]   Frisch, M. J.; Trucks, G. W.; Schlegel, H. B.; Scuseria, G. E.; Robb, M. A.; Cheeseman, J. R.; Montgomery, Jr., J. A.; Vreven, T.; Kudin, K. N.; Burant, J. C.; Millam, J. M.; Iyengar, S. S.; Tomasi, J.; Barone, V.; Mennucci, B.; Cossi, M.; Scalmani, G.; Rega, N.; Petersson, G. A.; Nakatsuji, H.; Hada, M.; Ehara, M.; Toyota, K.; Fukuda, R.; Hasegawa, J.; Ishida, M.; Nakajima, T.; Honda, Y.; Kitao, O.; Nakai, H.; Klene, M.; Li,

X.; Knox, J. E.; Hratchian, H. P.; Cross, J. B.; Bakken, V.; Adamo, C.; Jaramillo, J.; Gomperts, R.; Stratmann, R. E.; Yazyev, O.; Austin, A. J.; Cammi, R.; Pomelli, C.; Ochterski, J. W.; Ayala, P. Y.; Morokuma, K.; Voth, G. A.; Salvador, P.; Dannenberg, J. J.; Zakrzewski, V. G.; Dapprich, S.; Daniels, A. D.; Strain, M. C.; Farkas, O.; Malick, D. K.; Rabuck, A. D.; Raghavachari, K.; Foresman, J. B.; Ortiz, J. V.; Cui, Q.; Baboul, A. G.; Clifford, S.; Cioslowski, J.; Stefanov, B. B.; Liu, G.; Liashenko, A.; Piskorz, P.; Komaromi, I.; Martin, R. L.; Fox, D. J.; Keith, T.; Al-Laham, M. A.; Peng, C. Y.; Nanayakkara, A.; Challacombe, M.; Gill, P. M. W.; Johnson, B.; Chen, W.; Wong, M. W.; Gonzalez, C.; and Pople, J. A. <u>Gaussian 03 Revision C.02</u>. : Gaussian, Inc. Wallingford CT, 2004.

[52]   D.A. Case, T.A. Darden, T.E. Cheatham, III, C.L. Simmerling, J. Wang, R.E. Duke, R. Luo, K.M. Merz, D.A. Pearlman, M. Crowley, R.C. Walker, W. Zhang, B. Wang, S. Hayik, A. Roitberg, G. Seabra, K.F. Wong, F. Paesani, X. Wu, S. Brozell, V. Tsui, H. Gohlke, L. Yang, C. Tan, J. Mongan, V. Hornak, G. Cui, P. Beroza, D.H. Mathews, C. Schafmeister, W.S. Ross, and P.A. Kollman. <u>AMBER 9</u> : University of California, San Francisco, 2006.

[53]   J. Wang, R.M. Wolf, J.W. Caldwell, P.A. Kollamn and D.A. Case. Development and testing of a general Amber force field. <u>J. Comput. Chem.</u> 25 (2004) : 1157-1174.

[54]   H.J.C. Berendsen, J.R. Grigera and T.P. Straatsma. The missing term in effective pair potentials. <u>J. Phys. Chem.</u> 91 (1987) : 6269-6271.

[55]  S. Miyamoto and P.A. Kollman. SETTLE: An analytical version of the SHAKE and RATTLE algorithm for rigid water models. J. Comput. Chem. 13 (1992) :  952-962.

[56]  T. Darden, D. York and L. Pedersen. Particle mesh Ewald—an Nlog(N) method for Ewald sums in large systems. J. Chem. Phys. 98 (1993) : 10089-10092.

[57]  U. Essmann, L. Perera, M.L. Berkowitz, T. Darden, H. Lee and L.G. Pedersen. A smooth particle mesh Ewald method. J. Chem. Phys. 103 (1995) : 8577-8593.

[58]  Howard J. A. K., Hoy V. J., O'Hagan D., Smith G.T. How good is fluorine as a hydrogen bond acceptor? Tetrahedron 52 (1996) : 12613-12622.

# VITAE

**Name:** Uthumporn Arsawang

**Date of Birth:** May 6<sup>th</sup>, 1984

**Place of Birth:** Phichit, Thailand

**Nationality:** Thai

**e-mail address:** oi_piglet@hotmail.com

**Education:**

2002-2006    **B. Sc. in Mathematics**, Department of Mathematics, Faculty of Science, Chiang mai University, Chiang mai, Thailand.

2007-2009    **M.Sc. in Computational Science**, Department of Mathematics, Faculty of Science, Chulalongkorn University, Bangkok, Thailand.